A TWO-STAGE DETECTOR WITH IMPROVED ACCEPTANCE/REJECTION CAPABILITIES

Francesco Bandiera,[1] *Olivier Besson,*[2] *Danilo Orlando,*[1] *and Giuseppe Ricci*[1]

1: Dip. di Ing. dell'Innovazione
Università del Salento
Via Monteroni, 73100 Lecce, Italy
E-Mail: [francesco.bandiera, danilo.orlando, giuseppe.ricci]@unile.it

2: University of Toulouse, ISAE,
Dept. Electronics, Optronics and Signal
10 Avenue Edouard Belin
31055 Toulouse, France
E-Mail: besson@isae.fr

ABSTRACT

We propose a two-stage detector consisting of a Subspace Detector followed by the Whitened Adaptive Beamformer Orthogonal Rejection Test. The performance analysis shows that it possesses the Constant False Alarm Rate property with respect to the unknown covariance matrix of the noise and that it guarantees a wider range of directivity values with respect to previously proposed two-stage detectors. The probability of false alarm and the probability of detection (for both matched and mismatched signals) have been evaluated by means of numerical integration techniques.

Index Terms: radar detection, signal detection.

1. INTRODUCTION

In the last decades several papers have addressed adaptive radar detection of targets. Most of these papers follow the lead of the seminal paper by Kelly [1], where the Generalized Likelihood Ratio Test (GLRT) is used to conceive an adaptive decision scheme capable of detecting coherent pulse trains in presence of Gaussian disturbance with unknown covariance matrix. Training data, namely data with the same spectral properties of the noise in the cell under test, but supposed free of signals components, are used to estimate the unknown covariance matrix of the noise.

A significant amount of work has also been done in order to cope with mismatched signals. To this end, it is important to observe that a mismatched signal may arise due to several reasons as [2, 3]: 1) coherent scattering from a direction different to that in which the radar system is steered (sidelobe target); 2) imperfect modeling of the mainlobe target by the nominal steering vector, where the mismatch may be due to multipath propagation, array calibration uncertainties, beampointing errors, etc. Thus, it might be important to trade detection performance of mainlobe targets for rejection capabilities of sidelobe ones.

A detector with improved rejection capabilities is the Adaptive Beamformer Orthogonal Rejection Test (ABORT) [2]. The idea of ABORT is to modify the null hypothesis, which usually states that the vector under test contains noise only, so that it possibly contains a vector which, in some way, is orthogonal to the assumed target's signature. Doing so, if a signal with actual steering vector different from the nominal one is present, the detector will be less inclined to declare a detection. As customary, it is assumed that a set of training data is available at the receiver. The directivity of such detector is in between that of Kelly's detector, which, in turn, is more directive than the Adaptive Matched Filter (AMF) [4], and the one of the Adaptive Coherence Estimator (ACE) [5, 6]. However, in the original ABORT formulation, the fictitious signal is orthogonal to the nominal one in the *quasi-whitened* space, i.e., after whitening by the sample covariance matrix of the training samples. In [7], such an assumption was modified to address adaptive detection of distributed targets embedded in homogeneous disturbance, by resorting to the GLRT with the useful and the fictitious signals orthogonal in the *whitened* space, i.e., after whitening with the true covariance matrix. This modification leads to a detector, referred to in the following as Whitened ABORT (W-ABORT), with enhanced rejection capabilities of sidelobe signals; in fact, it may become even more selective than the ACE. On the other hand, increased robustness can be achieved by resorting to the tools of subspace detection, namely assuming that the target belongs to a known subspace of the observables.

Unfortunately, though, it seems difficult to find a decision scheme capable of providing at the same time good capabilities to reject sidelobe targets and high power in case of slightly mismatched mainlobe targets. In order to cope with this problem, the so-called two-stage detectors have been proposed; such schemes are formed by cascading two detectors (usually with opposite behaviors): the overall one declares the presence of a target in the data under test only when data under test survive both detection thresholdings. A rather famous two-stage detector is the Adaptive Sidelobe Blanker (ASB). The ASB has been proposed as a means to mitigate the high number of false alarms of the AMF in the presence of undernulled interference [8]. It can be seen as the cascade of the AMF and the ACE. Remarkably, it can adjust directivity by proper selection of the two thresholds in order to trade good rejection capabilities of sidelobe targets for acceptable detection loss of matched signals [8]. A further two-stage detector, consisting of the cascade of the AMF and Kelly's detector, has been proposed as a computationally efficient implementation of the latter [9]. More recently, the Subspace-based ASB (S-ASB) has been proposed [10]: it is obtained cascading a subspace GLRT-based detector (referred to in the following as subspace detector (SD)) and the ACE. The performance assessment has shown that proper thresholds setting can increase the robustness.

Herein, based upon the experience of [10], we propose a two-stage detector aimed at increasing also the selectivity of the S-ASB, i.e., its capability to reject mismatched signals. This is accomplished by cascading the SD and the W-ABORT. The performance assessment seems to confirm that its directivity varies in a wider range than its competitors, when we constrain the maximum loss with respect to Kelly's detector for matched signals, given the Probability of False Alarm (P_{fa}) and the Probability of Detection (P_d).

The work of O. Besson was supported by the Mission pour la Recherche et l'Innovation Scientifique (MRIS) of the Délégation Générale pour l'Armement (DGA) under grant no. 06-60-034.

2. PROBLEM FORMULATION

Assume that an array formed by N_a antennas senses the cell under test and that each antenna collects N_t samples. Denote by $\boldsymbol{z} \in \mathbb{C}^{N\times 1}$ the N-dimensional column vector, with $N = N_a N_t$, containing returns from the cell under test. We want to test whether or not $\boldsymbol{z}$ contains useful target echoes. As customary, we assume that a set of K training data, $\boldsymbol{z}_k \in \mathbb{C}^{N\times 1}$, $k = 1,\dots,K$, $K \geq N$, is available. The detection problem can be re-cast as

$$\begin{cases} H_0 : \boldsymbol{z} = \boldsymbol{n}, & \boldsymbol{z}_k = \boldsymbol{n}_k, \quad k = 1,\dots,K, \\ H_1 : \boldsymbol{z} = \alpha\boldsymbol{p} + \boldsymbol{n}, & \boldsymbol{z}_k = \boldsymbol{n}_k, \quad k = 1,\dots,K, \end{cases}$$

where

- $\boldsymbol{n}$ and the $\boldsymbol{n}_k \in \mathbb{C}^{N\times 1}$, $k = 1,\dots,K$, are independent and identically distributed complex normal random vectors with zero-mean and unknown covariance matrix $\boldsymbol{R}$, i.e., $\boldsymbol{n}, \boldsymbol{n}_k \sim \mathcal{CN}_N(\boldsymbol{0}, \boldsymbol{R})$, $k = 1,\dots,K$, with $\boldsymbol{R} \in \mathbb{C}^{N\times N}$ a positive definite covariance matrix;
- $\boldsymbol{p} \in \mathbb{C}^{N\times 1}$ is the direction of the (possible) mainlobe target echo, possibly different from that of the nominal steering vector $\boldsymbol{v} \in \mathbb{C}^{N\times 1}$;
- $\alpha \in \mathbb{C}$ is an unknown factor which accounts for both target and channel effects.

In the following we propose and assess a two-stage detector obtained by cascading the SD [11], whose statistic is given by

$$t_{\text{SD}} = \frac{\boldsymbol{z}^\dagger \boldsymbol{S}^{-1}\boldsymbol{H}(\boldsymbol{H}^\dagger \boldsymbol{S}^{-1}\boldsymbol{H})^{-1}\boldsymbol{H}^\dagger \boldsymbol{S}^{-1}\boldsymbol{z}}{1 + \boldsymbol{z}^\dagger \boldsymbol{S}^{-1}\boldsymbol{z}}, \tag{1}$$

and the W-ABORT, whose statistic is given by [7]

$$t_{\text{WA}} = \frac{1}{\left[\dfrac{|\boldsymbol{z}^\dagger \boldsymbol{S}^{-1}\boldsymbol{v}|^2}{(1+\boldsymbol{z}^\dagger \boldsymbol{S}^{-1}\boldsymbol{z})(\boldsymbol{v}^\dagger \boldsymbol{S}^{-1}\boldsymbol{v})} - 1\right]^2 (1 + \boldsymbol{z}^\dagger \boldsymbol{S}^{-1}\boldsymbol{z})}, \tag{2}$$

where

- † denotes conjugate transpose;
- $\boldsymbol{S} \in \mathbb{C}^{N\times N}$ is K times the sample covariance matrix of the secondary data, i.e., $\boldsymbol{S} = \boldsymbol{Z}\boldsymbol{Z}^\dagger$ with $\boldsymbol{Z} = [\boldsymbol{z}_1 \cdots \boldsymbol{z}_K] \in \mathbb{C}^{N\times K}$;
- $\boldsymbol{H} \in \mathbb{C}^{N\times r}$ is a full-column-rank matrix (and, hence, $r > 1$ is the rank of $\boldsymbol{H}$). Obviously, the choice of $\boldsymbol{H}$ will impact the performance of the overall detector; in order to guarantee reliable detection of mismatched mainlobe targets, it seems reasonable to set $\boldsymbol{H} = [\boldsymbol{v}\ \boldsymbol{v}_1]$ namely to consider a signal subspace spanned by the nominal steering vector and an additional one slightly mismatched with respect to $\boldsymbol{v}$. A deeper discussion on this point can be found in [10].

Notice that

$$t_{\text{K}} = \frac{|\boldsymbol{z}^\dagger \boldsymbol{S}^{-1}\boldsymbol{v}|^2}{(1+\boldsymbol{z}^\dagger \boldsymbol{S}^{-1}\boldsymbol{z})(\boldsymbol{v}^\dagger \boldsymbol{S}^{-1}\boldsymbol{v})}$$

is the well-known decision statistic of Kelly's detector [1].

Summarizing, the operation of the newly-proposed detector, referred to in the following as WAS-ASB, can be pictorially described as follows

$$\begin{array}{ccccc} t_{\text{SD}} \gtrless \eta & \xrightarrow{>\eta} & t_{\text{WA}} \gtrless \xi & \xrightarrow{>\xi} & H_1 \\ \downarrow <\eta & & \downarrow <\xi & & \\ H_0 & & H_0 & & \end{array},$$

where η and ξ form the thresholds pair to be set in order to guarantee the overall desired P_{fa}.

3. PERFORMANCE ASSESSMENT

In this section we derive analytical expressions for P_d and P_{fa} of the WAS-ASB; to this end, we replace t_{SD} with the equivalent decision statistic $\tilde{t}_{\text{SD}} = 1/(1 - t_{\text{SD}})$. Based upon results contained in [10, 12], it is possible to show that $\tilde{t}_{\text{SD}}$ and t_{WA} admit the following stochastic representations

$$\tilde{t}_{\text{SD}} = (\tilde{t}_{\text{K}} + 1)(1 + c), \quad t_{\text{WA}} = \frac{(\tilde{t}_{\text{K}} + 1)}{(1+b)(1+c)},$$

where $\tilde{t}_{\text{K}} = t_{\text{K}}/(1 - t_{\text{K}})$. Moreover, under the H_0 hypothesis, it is possible to show that [12]

- $\tilde{t}_{\text{K}}$, given b and c, is ruled by the central complex F-distribution with 1, $K - N + 1$ degrees of freedom (dof's);
- b is a central complex F-distributed random variable (rv) with $N - r$, $K - N + r + 1$ dof's, i.e., $b \sim \mathcal{CF}_{N-r,K-N+r+1}$;
- $c \sim \mathcal{CF}_{r-1,K-N+2}$ and it is independent of b.

Now, the P_{fa} of the two-stage detector can be expressed as

$$\begin{aligned} P_{fa} &= \mathrm{P}\left[t_{\text{SD}} > \eta, t_{\text{WA}} > \xi; H_0\right] = \mathrm{P}\left[\tilde{t}_{\text{SD}} > \tilde{\eta}, t_{\text{WA}} > \xi; H_0\right] \\ &= 1 - \int_0^{+\infty}\int_0^{+\infty} \mathcal{P}_0\left(\max\left(\frac{\tilde{\eta}}{1+\gamma} - 1,\right.\right. \\ &\quad \left.\left. \xi(1+\beta)(1+\gamma) - 1\right)\right) p_b(\beta) p_c(\gamma) d\beta d\gamma, \end{aligned}$$

where $\tilde{\eta} = 1/(1 - \eta)$, $p_b(\cdot)$ is the probability density function (pdf) of the rv b, $p_c(\cdot)$ is the pdf of the rv c, and $\mathcal{P}_0(\cdot)$ is the cumulative distribution function (CDF) of the rv $\tilde{t}_{\text{K}}$, given b and c (and under H_0), i.e., the CDF of a rv ruled by the $\mathcal{CF}_{1,K-N+1}$ distribution. It is now apparent that the WAS-ASB possesses the Constant False Alarm Rate (CFAR) property with respect to $\boldsymbol{R}$; in fact, the above expression of P_{fa} can be computed without knowledge of the noise covariance matrix $\boldsymbol{R}$.

Under the H_1 hypothesis, we assume a misalignment between the actual steering vector $\boldsymbol{p}$ and the nominal one $\boldsymbol{v}$, i.e., $\boldsymbol{p} \neq \boldsymbol{v}$. In this case, the rv's b and c depend on the mismatch angle. To be quantitative, let $\boldsymbol{x} = \boldsymbol{U}\boldsymbol{R}^{-1/2}\boldsymbol{z}$ where $\boldsymbol{U} \in \mathbb{C}^{N\times N}$ is a unitary matrix which rotates $\boldsymbol{H}_0$, a slice of unitary matrix obtained by means of QR factorization of the matrix $\boldsymbol{R}^{-1/2}\boldsymbol{H}$, into the first r elementary vectors[1], i.e.,

$$\boldsymbol{U}\boldsymbol{H}_0 = \begin{bmatrix} \boldsymbol{I}_r \\ \boldsymbol{0} \end{bmatrix};$$

in particular,

$$\boldsymbol{U}\boldsymbol{R}^{-1/2}\boldsymbol{v} = \sqrt{\boldsymbol{v}^\dagger \boldsymbol{R}^{-1}\boldsymbol{v}}\,\boldsymbol{e}_1,$$

with $\boldsymbol{e}_1$ the N-dimensional column vector whose first entry is equal to one and the remaining are zero. It turns out that the random vector $\boldsymbol{x}$ is distributed as [13]

$$\boldsymbol{x} \sim \mathcal{CN}_N\left(\alpha\sqrt{\boldsymbol{p}^\dagger \boldsymbol{R}^{-1}\boldsymbol{p}}\begin{bmatrix} e^{j\phi}\cos\theta \\ \boldsymbol{h}_{B_0}\sin\theta \\ \boldsymbol{h}_{B_1}\sin\theta \end{bmatrix}, \boldsymbol{I}_N\right),$$

where $\boldsymbol{h}_{B_0} \in \mathbb{C}^{(r-1)\times 1}$ and $\boldsymbol{h}_{B_1} \in \mathbb{C}^{(N-r)\times 1}$ are such that[2]

$$||\boldsymbol{h}_{B_0}||^2 + ||\boldsymbol{h}_{B_1}||^2 = 1$$

and

$$e^{j\phi}\cos\theta = \frac{\boldsymbol{v}^\dagger \boldsymbol{R}^{-1}\boldsymbol{p}}{\sqrt{\boldsymbol{p}^\dagger \boldsymbol{R}^{-1}\boldsymbol{p}}\sqrt{\boldsymbol{v}^\dagger \boldsymbol{R}^{-1}\boldsymbol{v}}}. \tag{3}$$

[1] $\boldsymbol{I}_m$ denotes the m-dimensional identity matrix.
[2] $||\cdot||$ denotes the Euclidean norm of a vector.

Moreover, since b and c depend upon θ we will denote these rv's by b_θ and c_θ . Due to the useful signal components, the distributions of $\tilde{t}_{\mathrm{K}}$, b_θ, and c_θ change; more precisely

- $\tilde{t}_{\mathrm{K}}$, given b_θ and c_θ, is ruled by the noncentral complex F-distribution with $1, K-N+1$ dof's and non-centrality parameter
$$\delta_\theta^2 = \frac{\mathrm{SNR}\cos^2\theta}{(1+b_\theta)(1+c_\theta)},$$
where $\mathrm{SNR} = |\alpha|^2 \boldsymbol{p}^\dagger \boldsymbol{M}^{-1}\boldsymbol{p}$ is the total available signal-to-noise ratio;
- b_θ is ruled by the noncentral complex F-distribution with $N-r, K-N+r+1$ dof's and non-centrality parameter
$$\delta_{b_\theta}^2 = \mathrm{SNR}\ \sin^2\theta\, ||\boldsymbol{h}_{B_1}||^2,$$
i.e., $b_\theta \sim \mathcal{CF}_{N-r,K-N+r+1}(\delta_{b_\theta})$;
- given b_θ, $c_\theta \sim \mathcal{CF}_{r-1,K-N+2}(\delta_{c_\theta})$, with
$$\delta_{c_\theta}^2 = \frac{\mathrm{SNR}\ \sin^2\theta\, ||\boldsymbol{h}_{B_0}||^2}{1+b_\theta}.$$

Thus, proceeding along the same line as for the derivation of the P_{fa}, it is easy to see that the P_d is given by

$$\begin{aligned} P_d &= 1 - \int_0^{+\infty}\int_0^{+\infty} \mathcal{P}_1\left(\max\left(\frac{\tilde{\eta}}{1+\gamma} - 1,\right.\right. \\ &\qquad \left.\left.\xi(1+\beta)(1+\gamma)-1\right)\right) p_{c_\theta|b_\theta}(\gamma|b_\theta=\beta)\, p_{b_\theta}(\beta)\, d\beta\, d\gamma, \end{aligned}$$

where $\mathcal{P}_1(\cdot)$ is the CDF of the rv $\tilde{t}_{\mathrm{K}}$, given b_θ and c_θ (and under H_1), i.e., the CDF of a rv ruled by the $\mathcal{CF}_{1,K-N+1}(\delta_\theta)$ distribution, $p_{b_\theta}(\cdot)$ is the pdf of a rv ruled by the $\mathcal{CF}_{N-r,K-N+r+1}(\delta_{b_\theta})$, and $p_{c_\theta|b_\theta}(\cdot|\cdot)$ is the pdf of a rv ruled by the $\mathcal{CF}_{r-1,K-N+2}(\delta_{c_\theta})$.

In the case of a perfect match between $\boldsymbol{v}$ and $\boldsymbol{p}$, i.e., $\theta = 0$, δ_{b_θ} and δ_{c_θ} are equal to zero, thus rv's c_θ and b_θ obey to the central complex F-distributions with $N-r, K-N+r+1$ and $r-1, K-N+2$ dof's, respectively. On the other hand, $\tilde{t}_{\mathrm{K}}$ is still subject to the noncentral complex F-distribution with $1, K-N+1$ dof's and non-centrality parameter given by

$$\delta_0^2 = \frac{\mathrm{SNR}}{(1+b_0)(1+c_0)}.$$

4. ILLUSTRATIVE EXAMPLES AND DISCUSSION

In this section we present some numerical examples to show the effectiveness of the WAS-ASB, also in comparison to the ASB and the S-ASB. All curves have been obtained by means of numerical integration techniques. In all examples the noise is modeled as an exponentially-correlated complex normal vector with one-lag correlation coefficient ρ, namely the (i,j)-th element of the covariance matrix $\boldsymbol{R}$ is given by $\rho^{|i-j|},\ i,j=1,\ldots,N$, with $\rho = 0.95$. The probability of false alarm is set to 10^{-4}. Moreover, we set $N_t = 1$, $N_a = N$, $r = 2$, and choose $\boldsymbol{v} = \boldsymbol{s}(0)$ and $\boldsymbol{v}_1 = \boldsymbol{s}(\pi/360)$ with

$$\boldsymbol{s}(\phi) = \frac{1}{\sqrt{N}}\left[1\ e^{j\frac{2\pi d}{\lambda}\sin\phi}\ \cdots\ e^{j(N-1)\frac{2\pi d}{\lambda}\sin\phi}\right]^T,$$

where d is the inter-element spacing, λ is the radar operating wavelength, and ^{T} denotes transpose. Moreover, we will denote by ϕ_T the azimuthal angle of the impinging useful target echo, i.e., $\boldsymbol{p} = \boldsymbol{s}(\phi_T)$. First, note that the P_{fa} of two-stage detectors depends on the two thresholds; as a consequence, there exist infinite thresholds pairs that guarantee the same value of P_{fa}. Fig. 1 shows the contour plots for the WAS-ASB corresponding to different values of P_{fa}, as functions of the thresholds pairs, $N = 16$, $K = 32$.

In Figs. 2-3 we plot P_d vs SNR for the S-ASB and the WAS-ASB, respectively, as they compare to Kelly's detector [1], for the case of a matched target, $N = 16$, $K = 32$; in these figures we show two curves (in addition to the curve of Kelly's detector) for each of them: such curves correspond to the limiting behaviors of the two-stage detectors for thresholds settings which guarantee $P_{fa} = 10^{-4}$. Fig. 2 shows that the maximum loss of the S-ASB with respect to Kelly's detector is less than (about) 1.2 dB (at $P_d = 0.9$); such a maximum loss increases to (about) 2 dB in Fig. 3 for the WAS-ASB.

In Figs. 4-6 we plot P_d vs ϕ_T (measured in degrees) for the ASB, the S-ASB, and the WAS-ASB, respectively, $N = 16$, $K = 32$; for all of the detectors plotted curves refer to thresholds pairs such that the loss for matched signals[3] with respect to Kelly's detector is less than (about) 1 dB at $P_d = 0.9$, $P_{fa} = 10^{-4}$. Observe from Figs. 4 and 5 that the S-ASB can ensure better robustness with respect to the ASB, due to the first stage (the SD), which is less sensitive than the AMF to mismatched signals. However, S-ASB and ASB exhibit the same capability to reject sidelobe targets, according to the fact that the second stage (the ACE) is the same. As it can be seen from Figs. 5 and 6, instead, the WAS-ASB can guarantee the same robustness of the S-ASB, but better rejection capabilities than the latter (and, consequently, better rejection capabilities than the ASB), due to the fact that the second stage has been replaced by the W-ABORT.

5. REFERENCES

[1] E. J. Kelly, "An Adaptive Detection Algorithm," *IEEE Trans. Aerosp. Electron. Syst.*, Vol. 22, No. 2, pp. 115-127, Mar. 1986.

[2] N. B. Pulsone and C. M. Rader, "Adaptive Beamformer Orthogonal Rejection Test," *IEEE Trans. Signal Process.*, Vol. 49, No. 3, pp. 521-529, Mar. 2001.

[3] G. A. Fabrizio, A. Farina, and M. D. Turley, "Spatial Adaptive Subspace Detection in OTH Radar," *IEEE Trans. Aerosp. Electron. Syst.*, Vol. 39, No. 4, pp. 1407-1427, Oct. 2003.

[4] F. C. Robey, D. L. Fuhrman, E. J. Kelly, and R. Nitzberg, "A CFAR Adaptive Matched Filter Detector," *IEEE Trans. Aerosp. Electron. Syst.*, Vol. 29, No. 1, pp. 208-216, Jan. 1992.

[5] E. Conte, M. Lops, and G. Ricci, "Asymptotically Optimum Radar Detection in Compound Gaussian Noise," *IEEE Trans. Aerosp. Electron. Syst.*, Vol. 31, No. 2, pp. 617-625, Apr. 1995.

[6] L. L. Scharf and T. Mc Whorter, "Adaptive matched subspace detectors and adaptive coherence estimators," in *Proc. of 30th Asilomar Conference Signals Systems Computers*, Pacific Grove, CA, USA, Nov. 3-6 1996, pp. 1114-1117.

[7] F. Bandiera, O. Besson, and G. Ricci, "An ABORT-like detector with improved mismatched signals rejection capabilities," *IEEE Trans. Signal Process.*, Vol. 56, No. 1, pp. 14-25, Jan. 2008.

[8] C. D. Richmond, "Performance of a Class of Adaptive Detection Algorithms in Nonhomogeneous Environments," *IEEE Trans. Signal Process.*, Vol. 48, No. 5, pp. 1248-1262, May 2000.

[9] N. B. Pulsone and M. A. Zatman, "A Computationally Efficient Two-Step Implementation of the GLRT," *IEEE Trans. Signal Process.*, Vol. 48, No. 3, pp. 609-616, Mar. 2000.

[10] F. Bandiera, D. Orlando, and G. Ricci, "A Subspace-based Adaptive Sidelobe Blanker," *IEEE Trans. Signal Process.*, under revision.

[11] E. J. Kelly and K. Forsythe, "Adaptive Detection and Parameter Estimation for Multidimensional Signal Models," Lincoln Lab, MIT, Lexington, Tech. Rep. No. 848, Apr. 19, 1989.

[3] The higher the threshold of the second stage the better the selectivity.

[12] F. Bandiera, O. Besson, D. Orlando, and G. Ricci, "An Improved Adaptive Sidelobe Blanker," *IEEE Trans. Signal Process.*, under revision.

[13] E. J. Kelly, "Adaptive detection in non-stationary interference-Part III," Massachusetts Institute of Technology, Lincoln Laboratory, Lexington, MA, Tech. Rep. 761, Aug. 1987.

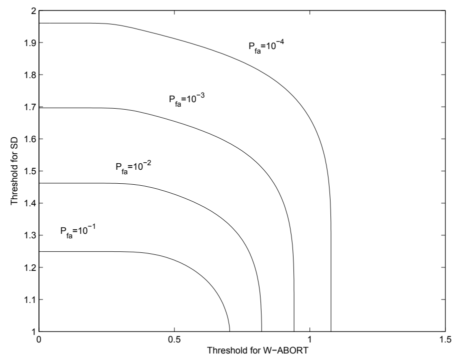

Fig. 1. Contours of constant P_{fa} for WAS-ASB with $N = 16$, $K = 32$, and $r = 2$.

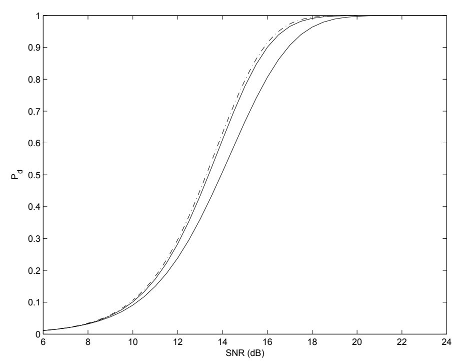

Fig. 2. P_d vs SNR for the S-ASB (solid lines) and the Kelly's detector (dash-dotted line) with $N = 16$, $K = 32$, and $r = 2$.

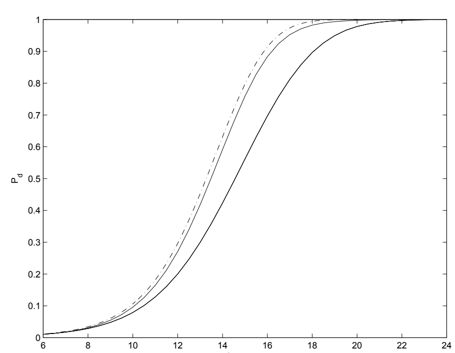

Fig. 3. P_d vs SNR for the WAS-ASB (solid lines) and the Kelly's detector (dash-dotted line) with $N = 16$, $K = 32$, and $r = 2$.

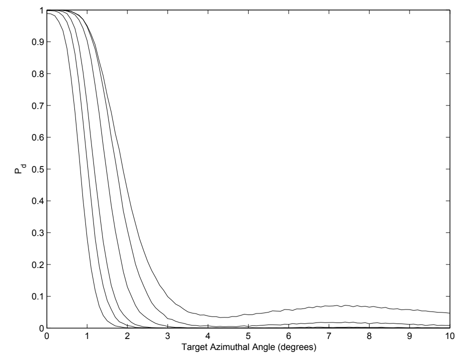

Fig. 4. P_d vs target azimuthal angle for the ASB with $N = 16$, $K = 32$, and SNR $= 19$ dB. Different curves refer to different thresholds pairs.

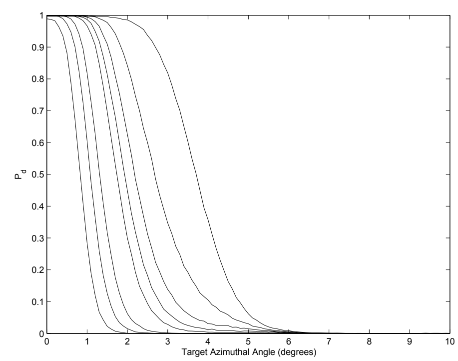

Fig. 5. P_d vs target azimuthal angle for the S-ASB with $N = 16$, $K = 32$, $r = 2$, and SNR $= 19$ dB. Different curves refer to different thresholds pairs.

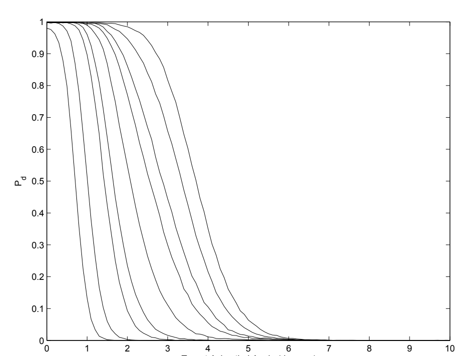

Fig. 6. P_d vs target azimuthal angle for the WAS-ASB with $N = 16$, $K = 32$, $r = 2$, and SNR $= 19$ dB. Different curves refer to different thresholds pairs.